

Selecting Very High Energy blazar as candidates for Cherenkov telescope observations by B-FlaP learning machine technique.

G.Chiaro,^{1,2,5}★ D.Salvetti,¹ G.La Mura² D.Bastieri^{1,5} and David J.Thompson⁴

²*Physics and Astronomy Dept. University of Padova Italy*

¹*Institute of Space Astrophysics and Cosmic Physics / INAF Milano Italy*

³*Institute of Radioastronomy, IRA, Bologna Italy*

⁴*NASA, Goddard Space Flight Center , Greenbelt MD USA*

⁵*Istituto Nazionale di Fisica Nucleare, Sez. di Padova, I-35131 Padova, Italy*

Accepted XXX. Received YYY; in original form ZZZ

ABSTRACT

Blazars and in particular their subclass High Synchrotron Peak (HSP) objects are the main targets of atmospheric Cherenkov telescopes. The present generation of Imaging Atmospheric Cherenkov Telescopes (IACTs), such as VERITAS, H.E.S.S. and MAGIC, has opened new frontiers of γ -ray astronomy in the Very High Energy range ($E > 100$ GeV). Since IACTs have a small field of view and observation take a lot of time, the ability to correctly identify TeV objects will be very important for the Cherenkov scientific community in the selection of targets, in order to save time and to increase the rate of detections. We used a learning machine technique to select Very High Energy candidates from the Fermi LAT 4-Year Point Source Catalog. The novelty of the present approach is that our study relies exclusively on photon flux collected at γ -ray energies where Fermi Large Area Telescope (LAT) is most sensitive (0.1 - 100 GeV) and the method remains totally independent of other information at different wavelengths.

Key words: keyword1 – keyword2 – keyword3

1 INTRODUCTION

Blazars are active galactic nuclei (AGN) with a radio-loud behavior and a relativistic jet pointing toward the observer. (?). These sources are divided into two main classes: BL Lacertae objects (BL Lacs) and Flat Spectrum Radio Quasars (FSRQ), which show very different optical spectra even if in other wavebands they are similar. FSRQs have strong, broad emission lines at optical wavelengths, while BL Lacs show at most weak emission lines, sometimes display absorption features, and can also be completely featureless. Blazars emit variable, non-thermal radiation across the whole electromagnetic spectrum, which includes two components forming two broad humps in a νf_ν representation. The low-energy one is attributed to synchrotron radiation, and the high-energy one is usually thought to be due to inverse Compton radiation. See ? for a recent review of the properties of γ -ray AGN. Blazars can also be classified into different subclasses based on the position

1 of the peak of the synchrotron bump in their spectral
2 energy distribution (SED), namely, low frequency peaked
3 (LSP or sources with $\nu_{peak}^S < 10^{14}$ Hz), intermediate
4 frequency peaked (ISP or sources with 10^{14} Hz $< \nu_{peak}^S$
5 $< 10^{15}$ Hz) and high frequency peaked (HSP or sources
6 with $\nu_{peak}^S > 10^{15}$ Hz) (?). BL Lac HSP sources are
7 the most numerous class of TeV sources (?). HSP are
8 ~30% of the sources listed in TeGeV catalog (?) which
9 collects all the information publicly available about the
10 TeV sources observed by the past and current generation
11 of imaging Cherenkov telescopes. ¹. Therefore the ability
12 to correctly identify new BL Lac HSP objects is very
13 interesting for the IACTs scientific community in order to
14 increase the number of known TeV sources as well as the
15 opportunity to increase the rate of detections, since IACTs
16 have a small field of view. For a recent review of present
17 and future Cherenkov telescopes, see ? and CTA project
18

★ E-mail: grazchiaro@gmail.com

¹ The catalog ASCII file can be retrieved from the *ASI Science Data Center*: <http://www.asdc.asi.it/tgevcatalog/index.php>.

<https://web.cta-observatory.org/> The aim of this study was focused in finding HSP blazar that might be reliable TeV candidates. For this purpose we used B-FlaP (?), hereinafter *Paper1*, a classification method of blazars based on a learning machine technique which relies exclusively on ECDF (Empirical Cumulative Distribution Function) of variability informations collected at γ -ray energies where *Fermi*-LAT space telescope (?) is most sensitive (0.1 – 100 GeV) and remains totally independent of other data at different wavelengths. In *Paper1* the method worked very well classifying , as BL Lac or FSRQ, 573 Blazar Candidates of Uncertain type (BCU) listed in The Third Catalog of Active Galactic Nuclei (?) (3LAC). This good result encouraged us to apply B-FlaP method in the search for new HSP TeV candidates in order to achieve the purpose of this study. See 3LAC for the counterpart conditions of BCUs. As first screening step In Fig 1 we plotted the ECDF for 3LAC blazar subclasses (right) and HSPs against FSRQs (left) . As we expected, because of the fact that HSP are almost exclusively represented by BL Lac objects (98.96%), the HSPs went through an FSRQ clean area at the upper left corner of the plot on the left. Even if the FSRQ (which are mainly ISP and LSP) contamination is not negligible, the result observed in Fig. 1 suggests *the potential ability* of B-FlaP to identify a flow range (less than $\sim 2.0 \times 10^{-8} \text{ ph cm}^{-2} \text{ s}^{-1}$) where it is possible to *suspect* the HSP subclass for a BCU source.

However, even here, visual inspection of the curves in all the ECDF figures shows that the shape of the curve does not show major differences between the observed blazar classes. Instead, a distinguishing factor is the γ flux found for any of the 48 monthly bin of the 3FGL flux history . We therefore focus our work on the possible use of the γ -ray flux as a distinguish parameter to help the HSP classification.

2 ARTIFICIAL NEURAL NETWORK TECHNIQUE

In order to find new BL Lac HSP candidates we used the B-FlaP algorithm developed in *Paper1*, based on the artificial neural network technique (ANN), which considered the empirical cumulative distribution function (ECDF) generated from the γ -ray light curves of the 3LAC classified blazars and BCU objects. The method considers flux values extracted from the distributions as predictor parameters and includes in the ANN algorithm γ -ray flux values corresponding to 10th, 20th, 30th, 40th, 50th, 60th, 70th, 80th, 90th and 100th percentile. This choice to use only 10 input parameters arised from a compromise between a good representation of each ECDF and to use a limited number of input parameters, in order to avoid problems related to upper limits associated to some time bins. The new feed-forward 2LP is built up of 10 input nodes, 5 hidden nodes and 2 output nodes. Using the B-FlaP method we chose as source sample all the 289 HSP and the 824 non-HSP identified by their spectral energy distribution and we compute the likelihood of a BCU sources to be an HSP. In this study we apply only one modification in B-FlaP original algorithm as lower classification threshold ($L_{HSP} > 0.8$) , in order to

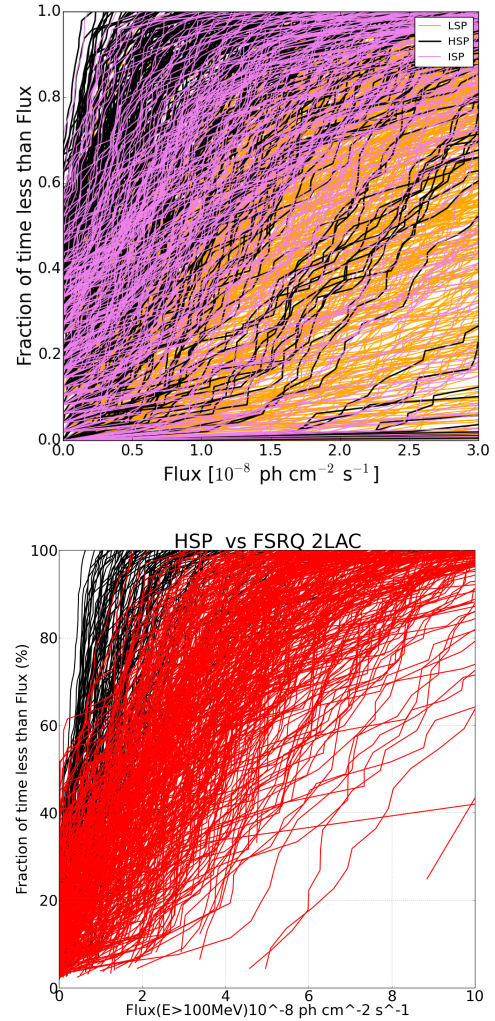


Figure 1. ECDF plots for blazars subclasses : (on left) LSP(orange) - ISP(purple) - HSP(black) , (on right) HPS vs FSRQ . The cumulative percentage of bins with flux below a given level is shown as a function of the 0.1 – 100 GeV flux in a bin, in units of $10^{-8} \text{ ph cm}^{-2} \text{ s}^{-1}$

increase the number of candidates, but at the expense of a smaller precision ($\sim 75\%$). In this way we improved the final result because the *sensitivity* increases to $\sim 15\%$ and the misclassified fraction of non-HSP remains very low ($\sim 2\%$).

Applying the optimized algorithm we selected 52 BCUs as the most promising HSP candidates. In Tab.1 we report the full list of HSP candidates. We compared our predictions with the broadband Spectral Energy Distributions (SED) available in 3LAC which provided an estimation of the synchrotron peak frequency ν_{peak}^S value extracted from a 3rd-degree polynomial fit of the low-energy hump of the SED. Classifications agree for $\sim 63\%$ of most promising HSP selected by ANN, validating the efficiency of our algorithm; disagree for $\sim 15\%$, in agreement with the expected contamination rate; and for the remaining $\sim 22\%$ ANN provides a classification as most promising HSP while the SED is not enough rigorous or available. As a further validation we com-

pare our HSP list with sources listed in 2WHSP catalog (?). 58% of the sources in our List are listed in 2WHSP catalog too. This confirms the previous result obtained by the comparison of the value at synchrotron peak frequency.

In order to obtain a narrow selection of TeV candidates for direct IACTs observation we refined the HSP selection through additional parameters which might better characterize the blazar TeV sources as following:

- γ -ray spectral photon index < 1.6
- Average significance over the 100 MeV to 300GeV energy band larger than 4.0 (Acero et al. 2015)

We used these additional threshold parameters because they reproduce some peculiar characteristics of TeV sources i.e. hard spectrum and significant brightness, as shown in the Second Catalog of Hard Fermi-LAT Sources (2FHL) (?) or TeV catalogs available in literature. For a usable sample from all three most important ground Cherenkov telescope : MAGIC, VERITAS and HESS , we selected only the sources which have favorable coordinates to grant their visibility at each observatory. Using these new parameters we reduced our first HSP selection from 52 to 16 sources (*clean list*)

For each source of the *clean list* we calculate the expected energy flux in the 50 GeV - 5 TeV energy range assuming that the spectral shape does not change to much compared to what the *Fermi*-LAT obtained in the range between 300 MeV and 100 GeV. We compute the expected energy flux using the following relation:

$$EFlux_{[50 \text{ GeV}-5 \text{ TeV}]} = \int_{50 \text{ GeV}}^{5 \text{ TeV}} \frac{dN}{dE} E dE \quad (1)$$

where dN/dE is the photon flux per unit energy, in units of $\text{cm}^{-2} \text{s}^{-1} \text{MeV}^{-1}$, derived from the spectral model that fits the data.

We use the best-fit model parameters included in the public *XML Model File* for LAT 4-year Point Source Catalog². In Fig.2 we report the python script used to compute the expected energy.

Tab.2 shows the *cleaned* list of HSP object identified as TeV candidates for IACTs. As a further control we compare the List in Tab.2 with the 2 FHL Catalog and we found that 6 of 16 sources are in both the lists. We called these sources Very High TeV candidates and we marked as VHT, or our best TeV candidates, in Tab.2. However we consider the remaining sources as interesting candidates that deserve particular attention in future IACT's observing campaigns.

2.1 Spectral Energy Distribution

Because of we expect an hard spectrum for a candidate at the TeV energies, the *Fermi* Energy Spectrum at 0.1- 100 GeV, might be an useful counterpart to our Artificial Neural Network prediction. Generally the TeV sources show an increasing slope of their energy spectrum with a maximum

around 100 GeV waiting for an average energy flux in the order of $10^{-11} dN/dE [\text{TeV}^{-1} \text{cm}^{-2} \text{s}^{-1}]$ at the TeV energies. This is the spectrum of the Crab Nebula, (?) and many other TeV observed sources. The Energy Spectrum of our TeV candidates listed in Tab.2 are fully consistent with these expected trends of the spectrum. In Figure 3 and Figure 4 we report the Energy Spectrum of the 6 VHT sources listed in Tab.2 . All of these have an hard slope as a suspected BL Lac candidate for potential emission in the TeV energy range. The whole list of 3FGL blazars Energy Spectrum can be retrieve from the ASI Science Data Center: <http://www.asdc.asi.it/fermi3fgl/>.

3 RESULTS AND CONCLUSIONS

In this Letter we confirm that, although a statistic method cannot replace rigorous spectroscopy as classification technique, using the improvement described in this paper the B-FlaP method and the variability informations might be configured as additional powerful approaches for a reliable identification of HSP blazars and TeV candidates when detailed observational or multiwavelength data are not yet available. In this study we classified 52 3FGL BCUs as BL Lac HSP sources and we selected 6 of them as Very High TeV candidate for IACTs observations. This result improve the knowledge of blazar population and could help for the Cherenkov scientific community to plan future observing campaigns.

ACKNOWLEDGEMENTS

Support for science analysis during the operations phase is gratefully acknowledged from the *Fermi*-LAT collaboration for making the 3FGL results available in such a useful form, the Institute of Space Astrophysics and Cosmic Physics of Milano -Italy (IASF INAF) and The Goddard Space Flight Center NASA. DS acknowledges support through EXTraS, funded from the European Commission Seventh Framework Programme (FP7/2007-2013) under grant agreement n. 607452.

² The file can be retrieved from the *Fermi* Science Support Center: http://fermi.gsfc.nasa.gov/ssc/data/access/lat/4yr_catalog/.

Table 1. Full HSP list selected from 3FGL BCUs

| 3FGLname | Assoc | Signif Avg | Spectral Ind. | B-FlaP Likelihood |
|-------------------|-----------------------|------------|---------------|-------------------|
| 3FGL J0030.2-1646 | 1RXS J003019.6-164723 | 9.160 | 1.647 | 0.981 |
| 3FGL J0039.0-2218 | PMN J0039-2220 | 4.411 | 1.715 | 0.984 |
| 3FGL J0040.3+4049 | B3 0037+405 | 6.379 | 1.132 | 0.996 |
| 3FGL J0043.5-0444 | 1RXS J004333.7-044257 | 5.840 | 1.735 | 0.984 |
| 3FGL J0043.7-1117 | 1RXS J004349.3-111612 | 5.896 | 1.594 | 0.993 |
| 3FGL J0047.9+5447 | 1RXS J004754.5+544758 | 5.042 | 1.334 | 0.995 |
| 3FGL J0132.5-0802 | PKS 0130-083 | 4.525 | 1.753 | 0.986 |
| 3FGL J0153.4+7114 | TXS 0149+710 | 7.056 | 1.567 | 0.992 |
| 3FGL J0204.2+2420 | B2 0201+24 | 5.146 | 1.792 | 0.983 |
| 3FGL J0305.2-1607 | PKS 0302-16 | 5.635 | 1.688 | 0.989 |
| 3FGL J0342.6-3006 | PKS 0340-302 | 4.729 | 1.846 | 0.986 |
| 3FGL J0439.6-3159 | 1RXS J043931.4-320045 | 6.437 | 1.771 | 0.988 |
| 3FGL J0506.9-5435 | 1ES 0505-546 | 14.856 | 1.603 | 0.991 |
| 3FGL J0515.5-0123 | NVSS J051536-012427 | 4.623 | 1.755 | 0.987 |
| 3FGL J0528.3+1815 | 1RXS J052829.6+181657 | 4.869 | 1.646 | 0.990 |
| 3FGL J0620.4+2644 | RX J0620.6+2644 | 5.032 | 1.65 | 0.987 |
| 3FGL J0640.0-1252 | TXS 0637-128 | 7.961 | 1.513 | 0.989 |
| 3FGL J0646.4-5452 | PMN J0646-5451 | 7.056 | 2.189 | 0.993 |
| 3FGL J0648.1+1606 | 1RXS J064814.1+160708 | 5.270 | 1.775 | 0.985 |
| 3FGL J0650.5+2055 | 1RXS J065033.9+205603 | 10.030 | 1.558 | 0.989 |
| 3FGL J0733.5+5153 | NVSS J073326+515355 | 6.251 | 1.741 | 0.989 |
| 3FGL J0742.4-8133 | SUMSS J074220-813139 | 4.518 | 1.464 | 0.995 |
| 3FGL J0746.9+8511 | NVSS J074715+851208 | 9.662 | 1.787 | 0.990 |
| 3FGL J0921.0-2258 | NVSS J092057-225721 | 4.101 | 1.553 | 0.994 |
| 3FGL J1040.8+1342 | 1RXS J104057.7+134216 | 4.887 | 1.76 | 0.989 |
| 3FGL J1141.2+6805 | 1RXS J114118.3+680433 | 7.089 | 1.611 | 0.993 |
| 3FGL J1155.4-3417 | NVSS J115520-341718 | 6.193 | 1.335 | 0.995 |
| 3FGL J1158.9+0818 | RX J1158.8+0819 | 5.428 | 1.869 | 0.981 |
| 3FGL J1203.5-3925 | PMN J1203-3926 | 7.312 | 1.639 | 0.989 |
| 3FGL J1319.6+7759 | NVSS J131921+775823 | 9.097 | 1.785 | 0.987 |
| 3FGL J1434.6+6640 | 1RXS J143442.0+664031 | 6.913 | 1.517 | 0.995 |
| 3FGL J1446.8-1831 | NVSS J144644-182922 | 4.179 | 1.723 | 0.987 |
| 3FGL J1547.1-2801 | 1RXS J154711.8-280222 | 4.285 | 1.708 | 0.982 |
| 3FGL J1612.4-3100 | NVSS J161219-305937 | 9.014 | 1.88 | 0.986 |
| 3FGL J1711.6+8846 | 1RXS J171643.8+884414 | 6.668 | 1.57 | 0.993 |
| 3FGL J1714.1-2029 | 1RXS J171405.2-202747 | 6.795 | 1.344 | 0.994 |
| 3FGL J1824.4+4310 | 1RXS J182418.7+430954 | 4.952 | 1.725 | 0.992 |
| 3FGL J1841.2+2910 | MG3 J184126+2910 | 8.353 | 1.567 | 0.989 |
| 3FGL J1855.1-6008 | PMN J1854-6009 | 4.206 | 1.813 | 0.987 |
| 3FGL J1908.8-0130 | NVSS J190836-012642 | 9.026 | 2.148 | 0.990 |
| 3FGL J1910.8+2855 | 1RXS J191053.2+285622 | 6.536 | 1.464 | 0.993 |
| 3FGL J1939.6-4925 | SUMSS J193946-492539 | 5.986 | 1.624 | 0.989 |
| 3FGL J1944.1-4523 | 1RXS J194422.6-452326 | 5.397 | 1.56 | 0.993 |
| 3FGL J1959.8-4725 | SUMSS J195945-472519 | 1.924 | 1.524 | 0.992 |
| 3FGL J2036.6-3325 | 1RXS J203650.9-332817 | 4.208 | 1.305 | 0.996 |
| 3FGL J2046.7-1011 | PMN J2046-1010 | 4.814 | 1.609 | 0.991 |
| 3FGL J2104.2-0211 | NVSS J210421-021239 | 4.060 | 1.524 | 0.993 |
| 3FGL J2108.6-8619 | 1RXS J210959.5-861853 | 4.729 | 1.74 | 0.990 |
| 3FGL J2312.9-6923 | SUMSS J231347-692332 | 4.931 | 1.804 | 0.989 |
| 3FGL J2316.8-5209 | SUMSS J231701-521003 | 5.606 | 1.735 | 0.988 |
| 3FGL J2347.9+5436 | NVSS J234753+543627 | 4.694 | 1.733 | 0.984 |

[ht!]

```
#!/usr/bin/env python

# these modules come with the standard Python
import argparse, sys, os, shutil
# reopen stdout to turn off the buffered output
sys.stdout = os.fdopen(sys.stdout.fileno(), 'w', 0)

# these modules are essential
import numpy as np

def main():
    # Energy range on where perform the integer
    emin = 5.e4 # MeV -> 50 GeV
    emax = 5.e6 # MeV -> 5 TeV
    delta = 10.

    #j0650
    n0 = 0.7261442133e-14
    pi = -1.558256791
    e0 = 0.9887826601e4

    flux = 0

    for e in np.arange(emin, emax, delta):
        flux += n0 * ((e / e0)**pi) * e * delta * 1.6022e-6

    print "Energia = %e erg/cm2/s" % flux

if __name__ == '__main__':
    main()
```

Figure 2. Python script used for TeV flux extrapolation

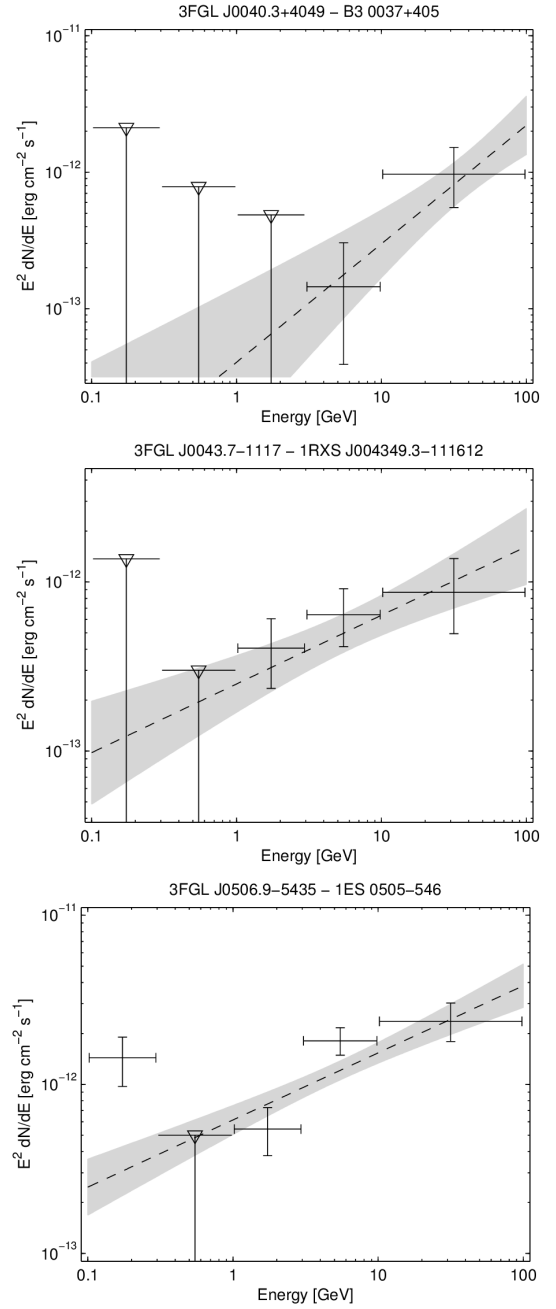


Figure 3.

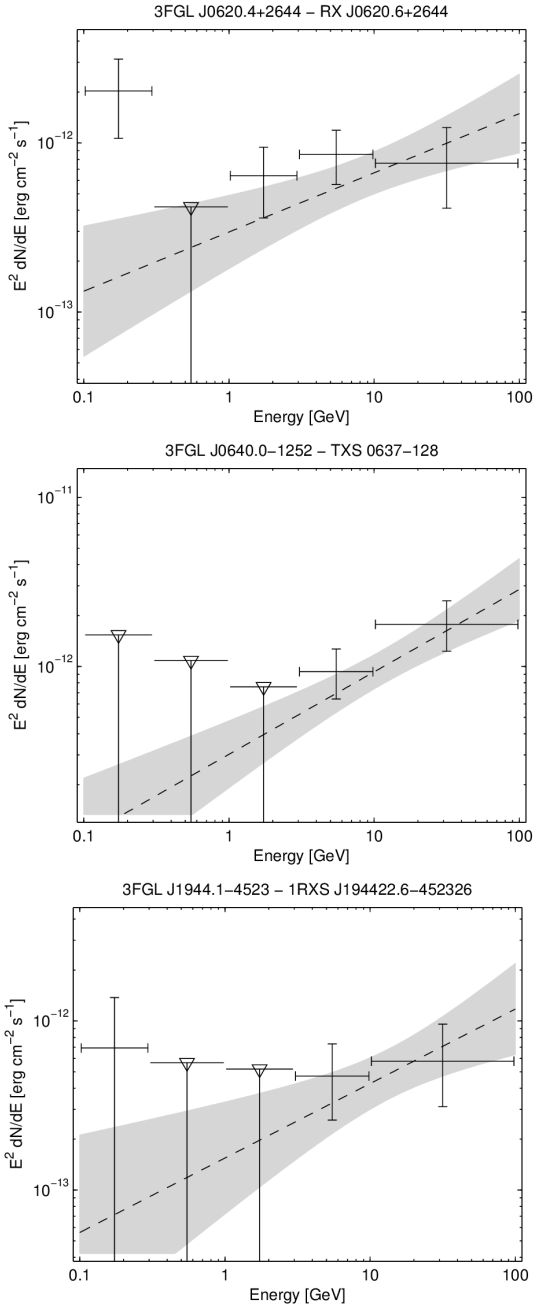


Figure 4. 0.1 - 100 GeV Energy Spectrum of 3FGL BCUs Very High candidates TeV and confirmed in 2FHL catalog

Table 2. Very High Candidates for IACTs telescopes

| VHTeV | 3FGLname | Assoc | RA | Dec | Signif Avg | Spectral Ind. | L B-Flap | 50GeV-5TeV E -11 |
|-------|-------------------|-----------------------|-------------|--------------|------------|---------------|----------|------------------|
| VHT | 3FGL J0040.3+4049 | B3 0037+405 | 00 43 44.4 | -11 17 17.08 | 6.379 | 1.132 | 0.996 | 7.432 |
| | 3FGL J1714.1-2029 | IRXS J171405.2-202747 | 17 14 07.9 | -20 29 46.6 | 6.795 | 1.344 | 0.994 | 7.098 |
| | 3FGL J2036.6-3325 | IRXS J203650.9-332817 | 20 36 41.8 | -33 25 36.8 | 4.208 | 1.305 | 0.996 | 4.036 |
| | 3FGL J1155.4-3417 | NVSS J115520-341718 | 11 55 26.8 | -34 17 57.4 | 6.193 | 1.335 | 0.995 | 3.863 |
| VHT | 3FGL J0506.9-5435 | IES 0505-546 | 05 06 58.3 | -54 35 01.28 | 14.856 | 1.603 | 0.991 | 3.828 |
| VHT | 3FGL J0640.0-1252 | TXS 0637-128 | 06 40 04.99 | -12 52 33.2 | 7.961 | 1.513 | 0.989 | 3.526 |
| | 3FGL J1841.2+2910 | MG3 J184126+2910 | 18 41 12.29 | +29 10 58.4 | 8.353 | 1.567 | 0.989 | 2.945 |
| | 3FGL J0030.2-1646 | IRXS J003019.6-164723 | 00 30 15.7 | -16 46 29.6 | 9.160 | 1.647 | 0.981 | 1.668 |
| VHT | 3FGL J0043.7-1117 | IRXS J004349.3-111612 | 00 43 44.4 | 11 17 17.08 | 5.896 | 1.594 | 0.993 | 1.652 |
| | 3FGL J1711.6+8846 | IRXS J171643.8+884414 | 17 11 37.9 | 88 46 26.0 | 6.668 | 1.57 | 0.993 | 1.609 |
| | 3FGL J2104.2-0211 | NVSS J210421-021239 | 21 04 12.29 | -02 11 27.2 | 4.060 | 1.524 | 0.993 | 1.541 |
| VHT | 3FGL J1203.5-3925 | PMN J1203-3926 | 12 03 31.6 | -39 25 31.4 | 7.312 | 1.639 | 0.989 | 1.525 |
| | 3FGL J0620.4+2644 | RX J0620.6+2644 | 06 20 28.99 | +26 44 22.19 | 5.032 | 1.65 | 0.987 | 1.340 |
| VHT | 3FGL J1944.1-4523 | IRXS J194422.6-452326 | 19 44 10.8 | -45 23 54.2 | 5.397 | 1.56 | 0.993 | 1.297 |
| | 3FGL J0921.0-2258 | NVSS J092057-225721 | 09 21 00.4 | -22 58 00.4 | 4.101 | 1.553 | 0.994 | 1.202 |
| | 3FGL J1141.2+6805 | IRXS J114118.3+680433 | 11 41 17.7 | +68 05 56.4 | 7.089 | 1.611 | 0.993 | 1.196 |

REFERENCES

| | |
|---|-----|
| REFERENCES | 192 |
| Abdo A. et al., 2011, ApJ, 716, 30 | 193 |
| Abdo A. A. et al. , 2011, ApJ, 716, 30 | 194 |
| Acero F. et al. , 2015, ApJS, 218, 23 | 195 |
| Acero F. et al., 2015, ApJ, 218, 23 | 196 |
| Ackermann et al., 2015, ApJ 810, 14, 34 | 197 |
| Ackermann et al., 2016, ApJ 222, 1, 5 | 198 |
| Alvarez Crespo N. et al. 2016 AJ, 151, 32 | 199 |
| Atwood W. B. et al., 2009, ApJ, 697, 1071 | 200 |
| Carosi A. et al., 2015, Proceeding of the 34th International Cosmic Ray Conference, p. 5 | 201 |
| Chang Y.L. et al. , 2016 in press arxiv 1609.05808 | 203 |
| Chiaro G. et al., 2016 MNRAS 462.3.3180C | 204 |
| De Naurois, M. et al., 2015, Comptes rendus - Physique, 16, 610 | 205 |
| Ghisellini G., 2013, EPJ Web of Conference, Vol. 61, id.05001. | 206 |
| Gish H., 1990, Proceeding on Acoustic Speech and Signal Processing, p. 1361 | 207 |
| Hillas A.M. et al., 1998,ApJ,503,744 | 209 |
| Horan D., Wakeley S., 2008, AAS, HEAD meeting 10, id.41.06 | 210 |
| Richard M. P., and Lippman R. P., 1991, Neural Computation, 3, 461 | 211 |
| | 212 |
| This paper has been typeset from a $\text{\TeX}/\text{\LaTeX}$ file prepared by the author. | 213 |
| | 214 |